ACS Macro Letters

pubs.acs.org/macroletters Letter

Reactivity-Guided Depercolation Processes Determine Fracture Behavior in End-Linked Polymer Networks

Haley K. Beech,[#] Shu Wang,[#] Devosmita Sen, Dechen Rota, Tatiana B. Kouznetsova, Akash Arora, Michael Rubinstein,* Stephen L. Craig,* and Bradley D. Olsen*

Cite This: *ACS Macro Lett.* 2023, 12, 1685–1691 Read Online

ACCESS | Metrics & More | Article Recommendations | Supporting Information

ABSTRACT: The fracture of polymer networks is tied to the molecular behavior of strands within the network, yet the specific molecular-level processes that determine the mechanical limits of a network remain elusive. Here, the question of reactivity-guided fracture is explored in otherwise indistinguishable end-linked networks by tuning the relative composition of strands with two different mechanochemical reactivities. Increasing the substitution of less mechanochemically reactive ("strong") strands into a network comprising more reactive ("weak") strands has a negligible impact on the fracture energy until the strong strand content reaches approximately 45%, at which point the fracture energy sharply increases with strong strand content. This aligns with the measured strong strand percolation threshold of 48 ± 3%, revealing that depercolation, or the loss of a percolated network structure, is a necessary criterion for crack propagation in a polymer network. Coarse-grained fracture simulations agree closely with the tearing energy trend observed experimentally, confirming that weak strand scissions dominate the failure until the strong strands approach percolation. The simulations further show that twice as many strands break in a mixture than in a pure network.

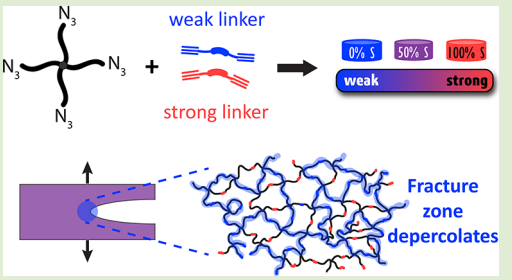

Rubbery polymeric networks are used in all facets of modern life, from tough elastomeric products such as tires or contact lenses to delicate, highly swellable gels used for precise drug delivery or tissue engineering.[1−3] Regardless of the application, premature failure can have consequences ranging from irritating to fatal. Understanding and predicting a fracture on the molecular level is an ongoing challenge due to a lack of quantitative correlation between single chain and bulk properties as well as yet unverified theoretical assumptions.[4−7] It is desirable to understand the nature of failure on the molecular level to begin to overcome these limitations.

In 1967, Lake and Thomas first proposed that the threshold tearing energy of elastomers, Γ_0, should be equal to the number of bridging strands per unit cross-section area multiplied by the energy stored per strand when a bridging strand breaks.[8] One key assumption often adopted is that the fracture zone, or the region at the crack tip within which strands are breaking and determine the tearing energy, is on the order of a single-chain end-to-end distance. While Lake and Thomas discussed the possibility of treating a larger fracture zone, in practice, their theory is often applied by assuming that the crack will follow a "simple path" across the material, breaking a single layer of chains. Likely because of its ease of implementation and qualitative success, this assumption has been used extensively in fracture literature, typically with an empirical enhancement factor to match experimental data.[8−14]

Contemporary studies have revealed that this assumption is often not sufficient to capture molecular behavior. Elegant prior work has examined crack propagation using mechanochemical reporter molecules incorporated in various types of polymer networks[15−19] and revealed that the damage zones in some networks are hundreds of microns up to several millimeters in width.[17,18,20] These results suggest that the crack is likely not a simple molecular path, such that considering a volume around the crack tip may be more realistic.

While many authors have recently proposed updated fracture theories that account for various types of topological defects,[13,21,22] most have maintained the simple path assumption. Arora et al. proposed a modified Lake Thomas theory that treats topological defects and re-examines the simple path assumption.[13] Their Micronetwork Fracture Theory (MFT) updated the fracture criterion to consider the fracture zone as a subnetwork that will fail when enough strands break to depercolate the network enclosed in the volume. The strand scission process and corresponding transition from continuous network to disparate fragments are termed depercolation to distinguish it from the forward process of network formation, although both share the same

Received: September 19, 2023
Revised: November 13, 2023
Accepted: November 15, 2023
Published: December 1, 2023

https://doi.org/10.1021/acsmacrolett.3c00559
ACS Macro Lett. 2023, 12, 1685−1691

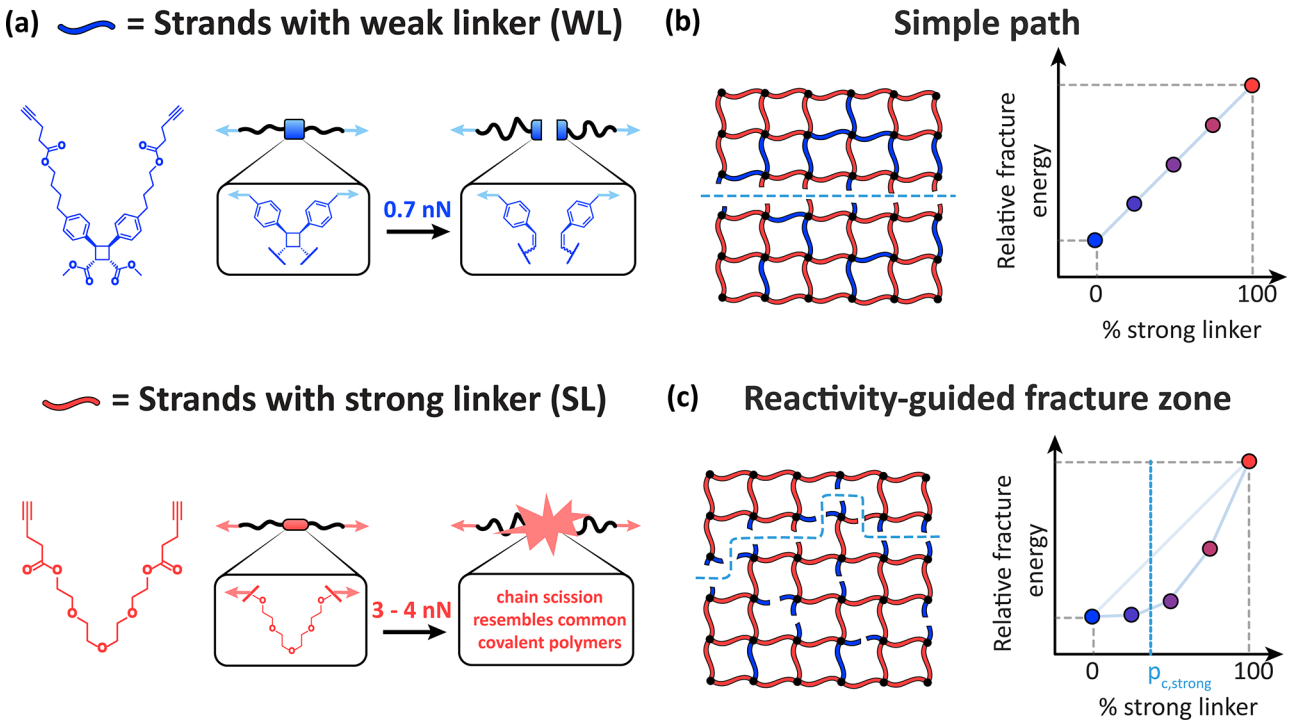

Figure 1. (a) Chemical structure and single molecule fracture behavior of the weak mechanophore (blue) and strong covalent (red) linkers. Hypothesized network fracture behavior and the corresponding trend expected in tearing energy for (b) the simple path, based on a lattice-based interpretation of the original Lake Thomas theory and (c) the reactivity-guided prediction where weak linkers are kinetically favored and fracture occurs when the fracture zone becomes depercolated.

percolation threshold. Depercolation occurs when $p < p_c$, where p is the fraction of intact strands and p_c is the percolation threshold.[13] The percolation threshold of a single-component network is commonly predicted with percolation theory[23−25] and was originally calculated by Flory[26] and Stockmayer[27] for a loop-free Cayley tree network. The distinguishing feature of MFT is that it treats a fracture zone much larger than a single layer of bridging strands, leading to qualitatively different tearing energy predictions.

As evidenced by the scope of recent experimental and theoretical fracture studies, many outstanding questions remain about the fundamental conceptualization of the crack itself: Should the crack path be considered as the rupture of a predefined set of polymer strands that bridge a simple cross-sectional plane or as a distributed set of events spread over a (variable) volume? To what extent do strand scission events occur outside of the minimum crack path? What processes govern crack propagation? And how does the molecular composition of a network influence those processes?

To begin to answer these questions, networks are cross-linked with varied ratios of "weak" and "strong" bis-alkyne linkers, as characterized via single molecule force spectroscopy (Figure 1a) to link microscopic network composition to macroscopic fracture behavior. Wang et al. previously embedded small-molecule mechanophores with varied force-coupled reactivities as linkers in the middle of polymer network strands in end-linked organogels.[28,29] These networks had identical connectivity but exhibited tearing energies that spanned a factor of 8 due to the specific mechanochemical strength of the network strands.[28] Each network consisted of a single type of linker, which suggested a direct correlation between the strand reactivities and the network mechanical strength.

Here, experimental data from networks of mixed reactivity are used to test the molecular behavior of crack propagation, while simulations lend further insight into fracture zone process details still out of reach with current experimental techniques. Existing molecular fracture models lead to different hypothesized outcomes. In the lattice-based simple path scenario, the crack proceeds across the material by cleaving the next strand on the path. This simple path approach assumes that chain scission occurs only along the crack plane. In a system of mixed-strand reactivities, the resulting tearing energies that would result are proportional to the statistical average of strong and weak strands, as shown in Figure 1b. Alternatively, molecular scission may be guided by their intrinsic mechanochemical reactivity, i.e., weak strands are more likely to break than strong strands. In this "reactivity guided" mechanism, the MFT predicts that the tearing energy should be relatively constant, favoring weak strand scission to depercolate the fracture zone with minimal strong strand cleavage. Above the percolation of strong strands, the number of strong strands that must break to depercolate the fracture zone will increase as the strong strand content increases, resulting in a qualitative tearing energy prediction shown in Figure 1c. As long as weak strands are favored to break in the fracture zone, the observed fracture energy is predicted to be below the simple path statistical average in networks of the same topology. These two hypotheses present simplified, testable scenarios that are probed in this work by varying the reactivity of the network strands.

To create mixed reactivity networks, bis-alkyne linkers were reacted with azide-functionalized 4-arm poly(ethylene glycol) (PEG, M_n = 5 kDa) via copper-catalyzed alkyne azide click (CuAAC) chemistry. The weak linker **WL** was a diaryl-substituted cyclobutane-based mechanophore, which is stable

https://doi.org/10.1021/acsmacrolett.3c00559
ACS Macro Lett. 2023, 12, 1685−1691

for more than 100 years in the absence of strain at room temperature, but undergoes a scissile cycloreversion reaction under external force (Figure 1a).[29] A force of ∼0.7 nN is required to reduce the half-life for cycloreversion to ∼0.25 s (Figure S1). The strong linker **SL** is tetraethylene glycol. Previous studies suggest that the polymer chain made from **SL** would break at the α C−C bond of the triazole group (pseudo benzylic position), which has a breaking force of >3 nN.[30] The gels were prepared at concentrations above overlap but well below the critical concentration for entanglement,[31] such that the tension along each elastically effective strand must be transmitted through the mechanochemical linkers. The linear viscoelastic properties of gels with each type of linker are consistent (Figure S2a). Loss moduli were also very close (Figure S2b) such that the viscoelastic dissipation should be similar for networks with either linker.

Tearing energies, obtained via the Thomas Rivlin method,[32] do not follow the simple path prediction as shown in Figure 2.

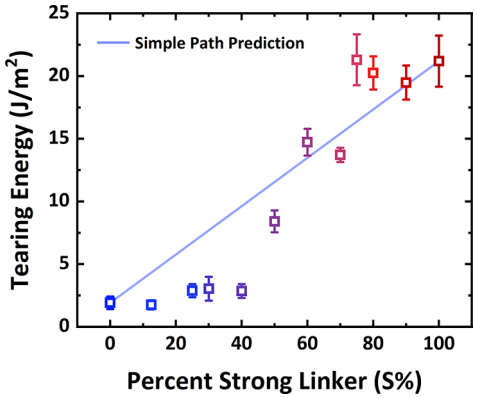

Figure 2. Tearing energy data as a function of the percentage of strong linker (S%) in tetra-PEG networks show that crack propagation is much more complex than the simple path assumption (blue line). Error bars represent standard error of the mean of five replicates.

The tearing energy remains constant when the percentage of strong linkers (S%) is below 40% ($\Gamma \approx 2$ J·m^{-2}) and above 75% ($\Gamma \approx 21$ J·m^{-2}). The quantitative tearing energy values are consistent with data previously reported on similar weak and strong mechanophore gels.[28] As the S% increases from 40% to 75%, an increase in the tearing energy from 2 to 21 J·m^{-2} was observed. While the initial plateau aligns with the reactivity-guided hypothesis, tearing energy in the high S% region surpasses the statistical average. This overshoot is not predicted by current molecular models, motivating subsequent studies with coarse-grained simulation.

The experimental percolation threshold was subsequently measured to compare with the onset of the tearing energy increase. A method of selective degradation was used to measure the depercolation threshold of fully formed gels by varying the ratio of cleavable to permanent linkers. Non-degradable counterparts for both the weak and the strong linkers, **WL′** and **SL′**, respectively, are shown in Figure 3a. The linear viscoelastic moduli of gels made with each of the linkers were identical within error (Figure S2a). Gels were made with a combination of **WL** and **SL′** for weak strand percolation and **SL** and **WL′** for strong strand percolation (Figure 3b). The gels reacted to high conversion (>99%, SI, section 4e), although defects are still present due to nonideal end-group functionality and conversion. Next, all of the cleavable bonds were degraded via basic hydrolysis, resulting in a homogeneous solution if the number of cleavable bonds was high enough to depercolate the network or a macroscopic gel if there were enough permanent bonds to maintain a percolated network, as demonstrated in Figure 3c. The interchangeability of the four linkers used for depercolation measurements was confirmed by consistent tearing energy across the degradable/nondegradable combinations (Figure S3). The percolation threshold for both weak and strong strands was measured at $p_c = 0.475 \pm 0.025$ (Figures S4 and S5), plotted for comparison to the experimental data in Figure 4a.

Coarse-grained fracture simulations were employed to obtain further mechanistic details of the failure process. The simulation first generates a network in real space via a Monte Carlo algorithm,[33] followed by tensile deformation steps using a kinetic Monte Carlo framework developed by Arora et al.,[13,34] updated here to allow for a bimodal population of strand types (details in SI, section 2b). Differences in bond reactivity are accounted for by modulating $U_{0,i}$, the bond dissociation energy of chain i, for each chain in the simulation. Stress−strain curves were generated for each replicate, from which toughness, W, was used as a representative comparison for fracture energy since the limited simulation box size prohibited the implementation of a notched sample equivalent. Simulation results were averaged over 20 individual runs and normalized across strong strand fractions for comparison to experimental tearing energy data as follows:

$$W_{norm} = \frac{W - W_{\min}}{W_{\max} - W_{\min}}$$

where min and max denote the minimum and maximum quantity observed across all S% ratios measured. Normalized experimental tearing energy is compared to simulated toughness in Figure 4a, with a trend across S% nearly identical with the experimental data.

To further verify the MFT depercolation hypothesis, the percolation threshold was calculated from the simulation with a computational analogue of the experimental approach. A specific number of strands were broken randomly throughout the simulation box, and the network was analyzed to determine whether it was still a gel (details in SI, section 2d). To compare directly to the experiment, the simulated percolation threshold was extrapolated to a thermodynamically large system size, yielding $p_c = 0.50 \pm 0.005$ (denoted by the dashed line in Figure 4a), within the error of the experimentally measured percolation threshold. Both the experimental and simulation percolation thresholds were considerably greater than the classical Flory−Stockmayer prediction of $p_c = 1/(f-1) = 1/3$. This is because Flory−Stockmayer theory does not account for any kind of cyclic structures which have been shown to substantially suppress the gel point.[35]

In contrast to experiments, individual strand-breaking events are readily extracted from simulation; the number of weak and strong strands in the simulation box that were broken during fracture (out of 10000 total) is plotted as a function of S% in Figure 4b. The data in plot Figure 4b are visualized in Figure 5, and both show the increase in total strand failure up to 70% S %, as well as the predominance of weak strand failure. More than 99% of failure events are weak strands for 0−40 S%; this proportion decreases very slightly to 98% immediately before strong strands percolate at 50 S%. Even when 90% of the

https://doi.org/10.1021/acsmacrolett.3c00559
ACS Macro Lett. 2023, 12, 1685−1691

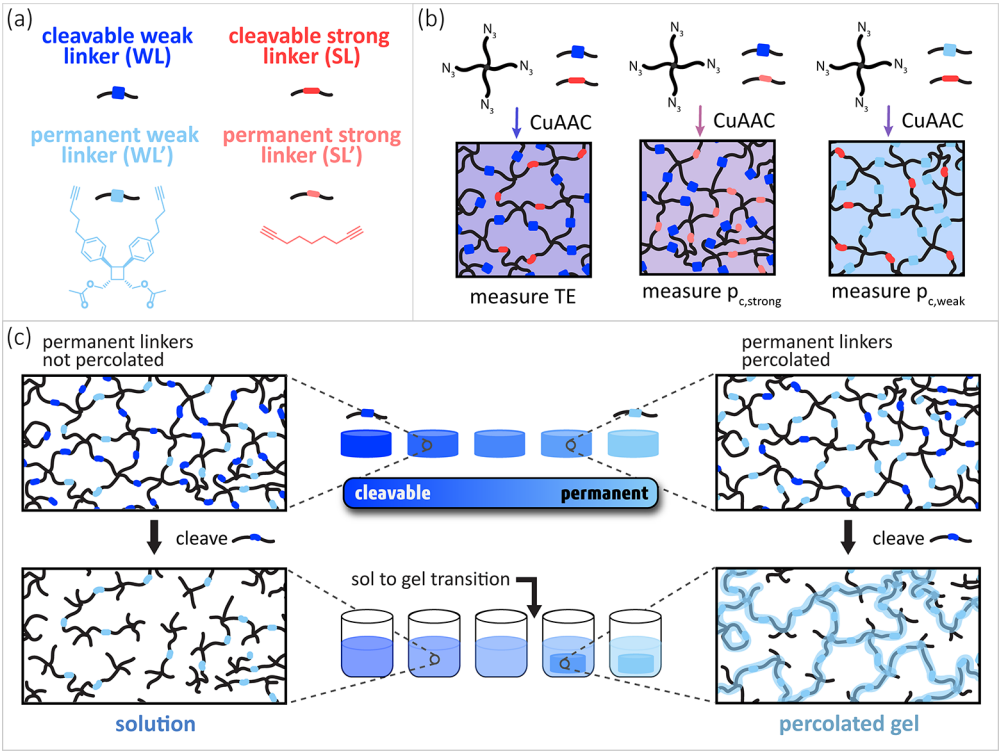

Figure 3. Experimental design to measure the depercolation threshold of a network. (a) Molecular structures of the nondegradable complements to **WL** and **SL**, **WL**′ and **SL**′, which were used in depercolation experiments. (b) Strong strand percolation was measured with **WL** and **SL**′, while weak strand percolation was measured with **SL** and **WL**′. (c) A series of gels with varied permanent bond content were synthesized, and the degradation of the cleavable bonds was used to determine the experimental sol-to-gel transition.

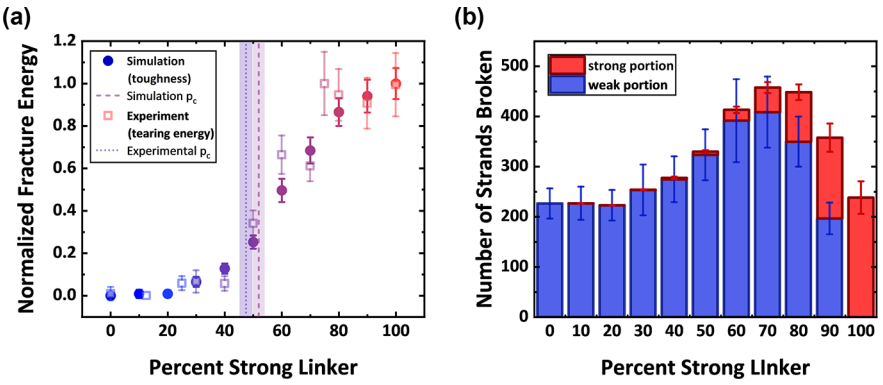

Figure 4. (a) Normalized fracture toughness extracted from coarse-grained simulations (circles) and experimental tearing energy (squares) as a function of linker composition demonstrates similar trends. (b) The number of weak (blue) and strong (red) strands in the simulation box broken before material failure is plotted as a function of S%. Simulation error bars were generated from 20 independent simulation replicates.

strands are strong, 55% of the strands that fail are weak. The increase in the total number of broken strands up to 70% S% is readily apparent both in Figure 4b and Figure 5a; not only do more strands break, but they appear to be more widely spread across the box.

The observed fracture behavior is markedly dependent on the composition of the linker reactivity in the sample. Before the simulated strong strand percolation threshold at 50% S%, more than 98% of broken strands are weak (Figure 4b), despite an increasing proportion of strong strands and strong strand connectivity. The close agreement between relative tearing energy in experiments and simulations suggests that this is also likely to be true in experiments, where the tearing energy is within the error of the pure weak linker network until 40% S%. Both simulation and experiment show a slight increase in the relative fracture energy before the corresponding percolation threshold that is mirrored by an increase in the total number of broken strands. This increase is likely due to more weak strand failure events to avoid chain scission within increasingly large clusters of strong strands as the S% increases. Analysis of strong strand clusters confirmed that the weight-average strong strand cluster degree of polymerization increased by an order of magnitude by 40% S% (SI, section 2f).

Over 70% of the total increase in fracture energy occurs in the intermediate region of strong strand composition from 50−75% S%. This region has the greatest number of broken strands and the largest spatial distribution of strand failure events. The high S% plateau above 75% S% observed in the

https://doi.org/10.1021/acsmacrolett.3c00559
ACS Macro Lett. 2023, 12, 1685−1691

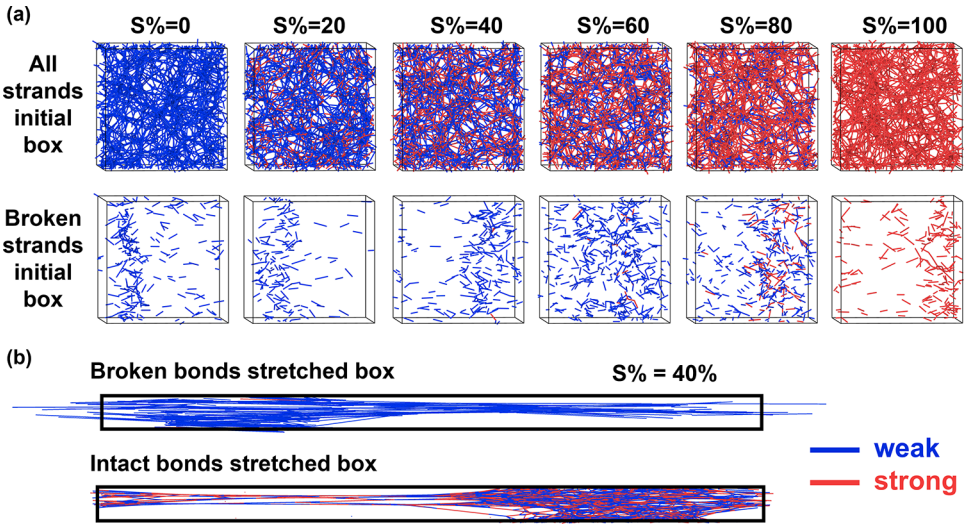

Figure 5. (a) Visualizations of the initial simulation box with all strands (top) and broken strands mapped back to the initial box (bottom). (b) Visualizations of the broken strands (top) and the remaining intact strands (bottom) in the simulation box for a 40% strong strand sample immediately before failure.

experiment is inconsistent with the purely reactivity-driven hypothesis put forth in Figure 1c. Fracture is fundamentally a kinetic process of chain scission governed by chain reactivity such that additional scission events (seen across the 60% and 80% S% simulation box in Figure 4a) could drive tearing energies to be greater than the energetic minimum. Due to the large difference between the force-dependent lifetime of the weak and strong strands coupled with the higher strain at break in these majority-strong strand samples (Figure S6), many weak strands which are not immediately within the crack plane experience enough force to break. The kinetic nature of crack failure is further evidenced by a sharp increase in strong strand failure events immediately before failure, while a sharp increase in weak strand failure events occurs at lower strains (Figure S7). These excess weak strand failure events may explain the unexpectedly large tearing energies, as extra weak strand failures dissipate energy, resulting in tearing energies greater than the predicted simple path average (blue line in Figure 2).

Crack propagation favors breaking the more reactive weak strands, even at the expense of breaking a greater total number of strands. Normalized experimental tearing energy results agree remarkably well with normalized toughness calculated from the simulation, demonstrating that the "sharpness" of the real crack is not so great as to influence where stress is focused. Both experimental and simulation results confirm that fracture of polymer gels will occur when the broken strand fraction surpasses the depercolation threshold, with the tearing energy remaining nearly invariant until the strong strands percolate. While this evidence supports a percolation process, there is not enough fidelity in the current data to intuit whether the percolation of the crack is classical or a more complex phenomenon such as invasion percolation, which includes dynamical considerations to favor the path of least resistance.[36] Simulation data demonstrate that the total number of broken strands varies as a function of the linker composition and that strand failure occurs across a wider region of the sample as the strong strand clusters become larger. The spatial increase in failure events does come at the cost of more total strands broken, resulting in higher-than-predicted tearing energy, as extraneous weak strand failure acts as a mechanism to dissipate energy.

In summary, these data support multiple fundamental insights into the molecular basis of network fracture in these systems: (a) that the depercolation of the fracture zone is a necessary criterion for crack propagation, as suggested by the micronetwork fracture theory; (b) that the distribution of molecular processes responsible for propagation is guided by the intrinsic reactivity of the components;[28] and (c) differences in the reactivity of network strands influence the total number of strands that break during fracture. These insights may also apply to networks with strands of different lengths. The findings have direct implications for fracture theories, which predominantly consider a single plane or constant volume zone for crack propagation regardless of strand chemistry or composition. This updated picture of fracture mechanics fundamentally shifts how fracture should be conceptually considered and can be used to inform modeling efforts and materials design.

■ ASSOCIATED CONTENT

Supporting Information

The Supporting Information is available free of charge at https://pubs.acs.org/doi/10.1021/acsmacrolett.3c00559.

Course-grained fracture simulation details and validation; Material synthesis routes; Material characterization methods and supporting data (PDF)

■ AUTHOR INFORMATION

Corresponding Authors

Bradley D. Olsen − *NSF Center for the Chemistry of Molecularly Optimized Networks, Duke University, Durham, North Carolina 27708, United States; Department of Chemical Engineering, Massachusetts Institute of Technology, Cambridge, Massachusetts 02139, United States;* orcid.org/0000-0002-7272-7140; Email: bdolsen@mit.edu

Stephen L. Craig − *NSF Center for the Chemistry of Molecularly Optimized Networks, Duke University, Durham, North Carolina 27708, United States; Department of Chemistry, Duke University, Durham, North Carolina*

https://doi.org/10.1021/acsmacrolett.3c00559
ACS Macro Lett. 2023, 12, 1685−1691

*27708, United States; orcid.org/0000-0002-8810-0369; Email: stephen.craig@duke.edu

Michael Rubinstein − *NSF Center for the Chemistry of Molecularly Optimized Networks, Duke University, Durham, North Carolina 27708, United States; Department of Chemistry and Departments of Mechanical Engineering and Materials Sciences, Biomedical Engineering, and Physics, Duke University, Durham, North Carolina 27708, United States*; Email: mr351@duke.edu

Authors

Haley K. Beech − *NSF Center for the Chemistry of Molecularly Optimized Networks, Duke University, Durham, North Carolina 27708, United States; Department of Chemical Engineering, Massachusetts Institute of Technology, Cambridge, Massachusetts 02139, United States;* orcid.org/0000-0003-3276-8578

Shu Wang − *NSF Center for the Chemistry of Molecularly Optimized Networks, Duke University, Durham, North Carolina 27708, United States; Department of Chemistry, Duke University, Durham, North Carolina 27708, United States;* orcid.org/0000-0001-7638-327X

Devosmita Sen − *NSF Center for the Chemistry of Molecularly Optimized Networks, Duke University, Durham, North Carolina 27708, United States; Department of Chemical Engineering, Massachusetts Institute of Technology, Cambridge, Massachusetts 02139, United States*

Dechen Rota − *NSF Center for the Chemistry of Molecularly Optimized Networks, Duke University, Durham, North Carolina 27708, United States; Department of Chemical Engineering, Massachusetts Institute of Technology, Cambridge, Massachusetts 02139, United States*

Tatiana B. Kouznetsova − *NSF Center for the Chemistry of Molecularly Optimized Networks, Duke University, Durham, North Carolina 27708, United States; Department of Chemistry, Duke University, Durham, North Carolina 27708, United States*

Akash Arora − *Department of Chemical Engineering, Massachusetts Institute of Technology, Cambridge, Massachusetts 02139, United States*

Complete contact information is available at: https://pubs.acs.org/10.1021/acsmacrolett.3c00559

Author Contributions

#These authors contributed equally (H.K.B. and S.W.).

Notes

The authors declare no competing financial interest.

■ ACKNOWLEDGMENTS

This work was supported by the NSF Center for the Chemistry of Molecularly Optimized Networks (MONET), CHE-2116298. We thank Prof. Jeremiah Johnson for insightful conversations. The authors acknowledge the MIT SuperCloud and Lincoln Laboratory Supercomputing Center for providing HPC and consultation resources that have contributed to the research results reported within this paper.

■ REFERENCES

(1) Flory, P. J. Network Structure and the Elastic Properties of Vulcanized Rubber. *Chem. Rev.* **1944**, *35* (1), 51−74.

(2) Hoare, T. R.; Kohane, D. S. Hydrogels in Drug Delivery: Progress and Challenges. *Polymer (Guildf).* **2008**, *49* (8), 1993−2007.

(3) Tibbitt, M. W.; Anseth, K. S. Hydrogels as Extracellular Matrix Mimics for 3D Cell Culture. *Biotechnol. Bioeng.* **2009**, *103* (4), 655−663.

(4) Dubach, F. F. C.; Ellenbroek, W. G.; Storm, C. How Accurately Do Mechanophores Report on Bond Scission in Soft Polymer Materials? *J. Polym. Sci.* **2021**, *59* (12), 1188−1199.

(5) Wang, S.; Panyukov, S.; Rubinstein, M.; Craig, S. L. Quantitative Adjustment to the Molecular Energy Parameter in the Lake-Thomas Theory of Polymer Fracture Energy. *Macromolecules* **2019**, *52*, 2772−2777.

(6) Stratigaki, M.; Göstl, R. Methods for Exerting and Sensing Force in Polymer Materials Using Mechanophores. *ChemPlusChem.* **2020**, *85*, 1095−1103.

(7) Danielsen, S. P. O.; Beech, H. K.; Wang, S.; El-Zaatari, B. M.; Wang, X.; Sapir, L.; Ouchi, T.; Wang, Z.; Johnson, P. N.; Hu, Y.; Lundberg, D. J.; Stoychev, G.; Craig, S. L.; Johnson, J. A.; Kalow, J. A.; Olsen, B. D.; Rubinstein, M. Molecular Characterization of Polymer Networks. *Chem. Rev.* **2021**, *121* (8), 5042−5092.

(8) Lake, G. J.; Thomas, A. G. The Strength of Highly Elastic Materials. *Proc. R. Soc. London Ser. A Math Phys. Sci.* **1967**, *300* (1460), 108−119.

(9) Ahagon, A.; Gent, A. N. Threshold Fracture Energies for Elastomers. *J. Polym. Sci. Polym. Phys. Ed.* **1975**, *13* (10), 1903−1911.

(10) Gent, A. N.; Tobias, R. H. Threshold Tear Strength of Elastomers. *J. Polym. Sci. Polym. Phys. Ed.* **1982**, *20* (11), 2051−2058.

(11) Akagi, Y.; Sakurai, H.; Gong, J. P.; Chung, U. Il; Sakai, T. Fracture Energy of Polymer Gels with Controlled Network Structures. *J. Chem. Phys.* **2013**, *139* (14), 144905.

(12) Sakai, T.; Akagi, Y.; Kondo, S.; Chung, U. Experimental Verification of Fracture Mechanism for Polymer Gels with Controlled Network Structure. *Soft Matter* **2014**, *10* (35), 6658−6665.

(13) Arora, A.; Lin, T.-S.; Beech, H. K.; Mochigase, H.; Wang, R.; Olsen, B. D. Fracture of Polymer Networks Containing Topological Defects. *Macromolecules* **2020**, *53* (17), 7346−7355.

(14) Lin, S.; Ni, J.; Zheng, D.; Zhao, X. Fracture and Fatigue of Ideal Polymer Networks. *Extrem. Mech. Lett.* **2021**, *48*, 101399.

(15) Degen, C. M.; May, P. A.; Moore, J. S.; White, S. R.; Sottos, N. R. Time-Dependent Mechanochemical Response of SP-Cross-Linked PMMA. *Macromolecules* **2013**, *46* (22), 8917−8921.

(16) Celestine, A. D. N.; Beiermann, B. A.; May, P. A.; Moore, J. S.; Sottos, N. R.; White, S. R. Fracture-Induced Activation in Mechanophore-Linked, Rubber Toughened PMMA. *Polymer (Guildf).* **2014**, *55* (16), 4164−4171.

(17) Matsuda, T.; Kawakami, R.; Nakajima, T.; Gong, J. P. Crack Tip Field of a Double-Network Gel: Visualization of Covalent Bond Scission through Mechanoradical Polymerization. *Macromolecules* **2020**, *53* (20), 8787−8795.

(18) Slootman, J.; Waltz, V.; Yeh, C. J.; Baumann, C.; Göstl, R.; Comtet, J.; Creton, C. Quantifying Rate-and Temperature-Dependent Molecular Damage in Elastomer Fracture. *Phys. Rev. X* **2020**, *10* (4), 41045.

(19) Chen, Y.; Sanoja, G.; Creton, C. Mechanochemistry Unveils Stress Transfer during Sacrificial Bond Fracture of Tough Multiple Network Elastomers. *Chem. Sci.* **2021**, *12* (33), 11098−11108.

(20) Dookhith, A. Z.; Lynd, N. A.; Creton, C.; Sanoja, G. E. Controlling Architecture and Mechanical Properties of Polyether Networks with Organoaluminum Catalysts. *Macromolecules* **2022**, *55* (13), 5601−5609.

(21) Lin, S.; Zhao, X. Fracture of Polymer Networks with Diverse Topological Defects. *Phys. Rev. E* **2020**, *102* (5), 52503.

(22) Wang, S.; Panyukov, S.; Craig, S. L.; Rubinstein, M. Contribution of Unbroken Strands to the Fracture of Polymer Networks. *Macromolecules* **2023**, *56*, 2309−2318.

(23) Stauffer, D.; Coniglio, A.; Adam, M. Gelation and Critical Phenomena. *Adv. Polym. Sci.* **1982**, *44*, 103−158.

(24) Stauffer, D.; Aharony, A. *Introduction to Percolation Theory*, 2nd revision; Taylor & Francis Inc.: Philadelphia, 1994.

(25) Rubinstein, M.; Colby, R. H. *Polymer Physics*; Oxford University Press: New York, 2003.

(26) Flory, P. J. Constitution of Three-Dimensional Polymers and the Theory of Gelation. *J. Phys. Chem.* **1942**, *46*, 132−140.
(27) Stockmayer, W. H. Theory of Molecular Size Distribution and Gel Formation in Branched-Chain Polymers. *J. Chem. Phys.* **1943**, *11* (2), 45−55.
(28) Wang, S.; Beech, H. K.; Bowser, B. H.; Kouznetsova, T. B.; Olsen, B. D.; Rubinstein, M.; Craig, S. L. Mechanism Dictates Mechanics: A Molecular Substituent Effect in the Macroscopic Fracture of a Covalent Polymer Network. *J. Am. Chem. Soc.* **2021**, *143* (10), 3714−3718.
(29) Bowser, B. H.; Wang, S.; Kouznetsova, T. B.; Beech, H. K.; Olsen, B. D.; Rubinstein, M.; Craig, S. L. Single-Event Spectroscopy and Unravelling Kinetics of Covalent Domains Based on Cyclobutane Mechanophores. *J. Am. Chem. Soc.* **2021**, *143* (13), 5269−5276.
(30) Smalø, H. S.; Uggerud, E. Ring Opening vs. Direct Bond Scission of the Chain in Polymeric Triazoles under the Influence of an External Force. *Chem. Commun.* **2012**, *48* (84), 10443−10445.
(31) Akagi, Y.; Gong, J. P.; Chung, U. Il; Sakai, T. Transition between Phantom and Affine Network Model Observed in Polymer Gels with Controlled Network Structure. *Macromolecules* **2013**, *46* (3), 1035−1040.
(32) Rivlin, R. S.; Thomas, A. G. Rupture of Rubber. I. Characteristic Energy for Tearing. *J. Polym. Sci.* **1953**, *10* (3), 291−318.
(33) Gusev, A. A. Numerical Estimates of the Topological Effects in the Elasticity of Gaussian Polymer Networks and Their Exact Theoretical Description. *Macromolecules* **2019**, *52*, 3244−3251.
(34) Arora, A.; Lin, T.-S.; Olsen, B. D. Coarse-Grained Simulations for Fracture of Polymer Networks: Stress Versus Topological Inhomogeneities. *Macromolecules* **2022**, *55* (1), 4−14.
(35) Wang, R.; Lin, T.-S.; Johnson, J. A.; Olsen, B. D. Kinetic Monte Carlo Simulation for Quantification of the Gel Point of Polymer Networks. *ACS Macro Lett.* **2017**, *6*, 1414−1419.
(36) Wilkinson, D.; Willemsen, J. F. Invasion Percolation: A New Form of Percolation Theory. *J. Phys. A. Math. Gen.* **1983**, *16* (14), 3365−3376.

https://doi.org/10.1021/acsmacrolett.3c00559
ACS Macro Lett. 2023, 12, 1685−1691